Published in final edited form as:
Cell Calcium. 2007 June ; 41(6): 559–571. doi:10.1016/j.ceca.2006.10.006.

Ca^{2+} signal summation and NFATc1 nuclear translocation in sympathetic ganglion neurons during repetitive action potentials

Erick O. Hernández-Ochoa, **Minerva Contreras**, **Zoltán Cseresnyés**, and **Martin F. Schneider***
Department of Biochemistry and Molecular Biology, School of Medicine, University of Maryland. Baltimore, MD 21201

Abstract

NFATc-mediated gene expression constitutes a critical step during neuronal development and synaptic plasticity. Although considerable information is available regarding the activation and functionality of specific NFATc isoforms, in neurons little is known about how sensitive NFAT nuclear translocation is to specific patterns of electrical activity. Here we used high-speed fluo-4 confocal imaging to monitor action potential (AP)-induced cytosolic Ca^{2+} transients in rat sympathetic neurons. We have recorded phasic and repetitive AP patterns, and corresponding Ca^{2+} transients initiated by either long (100–800 ms) current-clamp pulses, or single brief (2 ms) electrical field stimulation. We address the functional consequences of these AP and Ca^{2+} transient patterns, by using an adenoviral construct to express NFATc1-CFP and evaluate NFATc1-CFP nuclear translocation in response to specific patterns of electrical activity. 10 Hz train stimulation induced nuclear translocation of NFATc1, whereas 1 Hz trains did not. However, 1 Hz train stimulation did result in NFATc1 translocation in the presence of 2 mM Ba^{2+}, which inhibits M-currents and promotes repetitive firing and the accompanying small (~ 0.6 $\Delta F/F_0$) repetitive and summating Ca^{2+} transients. Our results demonstrate that M-current inhibition-mediated spike frequency facilitation enhances cytosolic Ca^{2+} signals and NFATc1 nuclear translocation during trains of low frequency electrical stimulation.

Keywords

Adaptation; Facilitation; Ca^{2+} transients; NFATc; Action potential; sympathetic; neurons

1. Introduction

Ca^{2+} signaling, a critical and common form of intracellular communication in both neuronal and non-neuronal cell types, employs a wide array of effectors to regulate many distinct cellular processes, from cell excitability to gene expression [1]. Nuclear factor of activated T cells (NFATc1–4) proteins are members of a family of transcription factors exhibiting Ca^{2+}-dependent activation, which is regulated by calcineurin, a Ca^{2+}-dependent phosphatase [2]. After a rise in intracellular Ca^{2+}, NFATc are dephosphorylated by calcineurin in the

*To whom correspondence should be addressed, **Martin F. Schneider.**, Department of Biochemistry and Molecular Biology, School of Medicine, University of Maryland, Baltimore, 108 N. Greene Street, Baltimore, MD 21201, Telephone: 410-706-7812, FAX: 410-706-8297, mschneid@umaryland.edu.

cytoplasm, thereby promoting their translocation from the cytosol into the nucleus to initiate transcription [2, 3]. In neurons, activation of specific NFATc family members has been demonstrated during electrical activity [4]. NFATc-mediated gene expression has been proposed as a key step during neuronal morphogenesis and development, synaptic plasticity and neuronal function [4, 5, 6].

Many neurons, including sympathetic neurons, respond to a constant suprathreshold electrical stimulus with a gradual reduction of the firing frequency (spike-frequency adaptation; SFA). Among the large variety of mechanisms responsible for SFA, M-type K^+ currents [7, 8] are of particular importance [9]. Under certain conditions (e.g. during inhibition of the M-current by neurotransmitters and neuropeptides or by using M-channel blockers) SFA can be reversed [7, 8, 10], resulting in spike frequency facilitation (SFF). Adaptation induced by ionic currents, or facilitation resulting from their inhibition may strongly impact neuronal functions.

In the current study, we examined the effects of SFA and SFF on the pattern of Ca^{2+} transients and on the activation and nuclear translocation of the NFATc1 during specific patterns of electrical stimulation in rat sympathetic neurons. We now provide evidence that SFF enhances NFATc1 nuclear translocation during low frequency stimulation.

2. Material and Methods

2.1. Cell culture

Superior cervical ganglion (SCG) neurons were enzymatically dissociated from 5-weekold male Wistar rats as described elsewhere [11]. Briefly, rats were placed in a container and exposed to rising concentrations of CO_2. The animals were sacrificed according to authorized procedures of the Institutional Animal Care and Use Committee, University of Maryland Baltimore (Baltimore, MD). After dissection, the ganglia were desheathed, cut into eight to ten small pieces and enzymatically dissociated with papain for 20 min and then with collagenase type I and dispase type II for 40 min. Individual neurons were released by trituration and then plated on poly-L-lysine coated glass coverslips in culture dishes and stored in a humidified atmosphere of 95% air 5% CO_2 at 37°C in Dulbecco's modified Eagle's medium (DMEM) supplemented with fetal bovine serum and penicillin-streptomycin. Neurons were studied 1 to 6 days after plating.

2.2. High-speed confocal imaging and field stimulation

Confocal imaging experiments were carried out on a Zeiss LSM 5 Live system, based on an Axiovert 200M inverted microscope. To evaluate temporal properties of Ca^{2+} signals, cells were loaded with 2 μM fluo-4AM in a mammalian Ringers' solution (containing mM: 160 NaCl, 3 KCl, 2 $CaCl_2$, 10 HEPES, 8 glucose, 1 $MgCl_2$, 0.1 EGTA; pH 7.4 with NaOH) at room temperature for 20 minutes and then washed three times with 2mL of dye-free Ringer's solution. In separate experiments, we used annine-6, a fast response membrane voltage sensitive dye. Annine-6 was dissolved in DMSO and sonicated for 15 min before the experiment. Cells were stained with 10 μM annine-6 in Ringer's solution for 30 minutes and then washed. Cells were imaged with a 63X NA 1.2 water immersion objective lens. Excitation for both fluo-4 and annine-6 was provided by the 488 nm line of a 100 mW diode laser, and emitted light was collected at > 510 nm. Principal SCG neurons were selected for Ca^{2+} experiments based on their size (> 20 μM in diameter). To change the voltage across the cell membrane we applied a 1–2 ms extracellular field stimulus. This method has some disadvantages (see Discussion), but is much simpler than whole-cell patch-clamp recordings. Use of field stimulation provided a quick way to identify firing patterns in a large number of neurons. Two parallel platinum wires approximately 5 mm apart were

positioned at the bottom of the dish in order to apply the electrical field. The voltage stimuli were timed by a waveform generator and delivered using a custom high output-current stimulator. To minimize electrolysis at the electrodes, every other applied voltage waveform was of reversed polarity. Application of each pulse protocol was synchronized to the start of the confocal scan. Typically, the field stimulus was applied several milliseconds (indicated in each figure) after the start of the confocal scan sequence, thus providing control images prior to stimulation at the start of each sequence. These control images were used to determine the resting steady-state fluorescence level (F_0).

2.3. Electrophysiology

Membrane potential measurements were performed in the whole-cell configuration of the patch-clamp technique [12] using an EPC-10 amplifier (HEKA Instruments Inc., Germany). Current-clamp experiments were carried out using Ringer's solution and an intracellular pipette solution containing (in mM): 150 KCl, 7 NaCl, 4 $MgCl_2$, 5 Na_2ATP, 14 phosphocreatine-Na_2, 0.3 Na_2GTP, 10 HEPES. (pH 7.2). In some cases, the patch was perforated by adding 0.15 mM of nystatin to the pipette solution [13]. During Ca^{2+} channel current recordings, the bath solution contained (in mM): 162.5 TEA-Cl, 2 $CaCl_2$, 10 HEPES, 8 glucose, 1 $MgCl_2$, 0.001 TTX, pH adjusted to 7.4 with TEA-OH. The pipette solution (internal solution) contained (in mM): 140 CsCl, 10 HEPES, 1 $CaCl_2$, 5 MgCl2, 5 Na_2ATP, 0.3 Na_2GTP and 0.1 leupeptin, pH adjusted to 7.4 with CsOH. The sampling frequency was 10 kHz (filtered at 3 kHz). Data were acquired, stored, analyzed and plotted using Patchmaster, Fitmaster (HEKA Instruments Inc.) and Origin 7.5 software (OriginLab Corporation, Northampton, MA, USA). For M-type K^+ channel current (I_M) measurements the external solution was modified to (in mM): 162.5 NaCl, 2.5 KCl, 5 CaCl2, 1 MgCl2, 10 HEPES, 10 Glucose and 0.001 TTX, pH adjusted to 7.4 with NaOH. The pipette solution contained (in mM): 175 KCl, 5 $MgCl_2$, 10 HEPES, 0.5 EGTA, 5 Na_2ATP, 0.3 Na_2GTP and 0.1 leupeptine, pH adjusted to 7.4 with KOH. I_M was activated by setting the holding potential to −25 mV, whereas I_M was deactivated by 800 ms command pulses from −25 mV to −60 mV, applied every 4 s. The M-type K^+ current deactivation amplitude and its relative inhibition were measured as the difference between the current at 10–20 ms after the beginning of voltage step (at −60 mV), and the current at the end of the voltage step.

2.4. Adenoviral infection and image analysis of nuclear translocation of NFATc1

The construction of recombinant adenoviruses of NFATc1-CFP or CFP were described in detail previously [14]. The virus infection (~7×10^{11} particles/mL) was carried out ~48 h after the neurons were plated. 24–48 hrs after the adenoviral infection, the culture medium was changed to Ringers' solution. Confocal images were acquired on an Olympus Fluoview FV500 system based on an inverted Olympus IX/70 microscope. The culture dish was mounted on a computer controlled motorized stage and cells were imaged with a 60X NA 1.4 water immersion objective lens. Excitation for CFP was provided by the 440 nm line of a diode laser, and the emitted light was collected between 465 and 495 nm. Two stimulation protocols were used: 1) a 5 s train of *1 Hz* stimuli once every 50 s, and 2) a 5 s train of *10 Hz* stimuli every 50 s. Confocal images were acquired sequentially before and after 20–40 minutes of stimulation in order to record NFATc1-CFP translocation.

2.5. RT-PCR for NFAT Isoforms

Using data bank sequences for mouse, human and rat NFATc1, 2, 3 and 4, we designed PCR primers, each spanning one intron, for each of the rat NFAT isoforms. Primers for each isoform were selected in regions conserved between mouse and rat species but outside of the consensus rel and IPT domains to insure isoform specificity. RNA was isolated from homogenized superior cervical ganglia using Trizol, whereas RT-PCR (both Invitrogen) was used to identify isoform specific transcripts.

2.6. Drugs and Chemicals

All drugs and chemicals used in this study were purchased from Sigma, except fluo-4-AM (Molecular Probes, Eugene, OR) and annine-6 (Hinner & Adleff & Komenda & Dr. Hubener Sensitive Farbstoffe GbR, Munich, Germany).

2.7. Data analysis

Average intensity of fluorescence within selected small (generally 12–16 μm^2) areas of interest (AOIs) was measured using software custom-written in the IDL programming language (Research Systems, Inc.). Images in x-y mode (frame sizes: 512 × 200 or 512 × 30 pixels; respective scan speeds: 108 or 732 fps; 19.77 or 19.19 μs/line, respectively) were background corrected by subtracting an average value recorded outside the cell. The average fluorescence value before electrical stimulation (F_0) was used to scale Ca^{2+} and voltage signals as $\Delta F/F_0$. The averages were given as mean ± SEM and statistical significance was assessed using the Student's t-test at a P level of 0.05. All the experiments were conducted at room temperature (20–24° C).

3. Results

3.1. Trains of repetitive Ca^{2+} transients in response to a single brief field stimulus in cultured SCG neurons

In many of the neurons tested in 24 hr old cultures, a single brief (2 ms) electrical field stimulus induced a single, rapidly rising, more slowly decaying Ca^{2+} transient that was similar in areas of interest (AOIs) around the periphery of the neuron (Figure 1, A). In other cells in the same 24 hr cultures, the same 2 ms stimulus unexpectedly elicited a *train* of rapidly rising, more slowly decaying and partially summating intracellular Ca^{2+} transients (Figure 1 B). Additional data, presented below, indicates that each of the Ca^{2+} transients in the partially summating train of Ca^{2+} signals is initiated by one action potential in a corresponding train of action potentials. The different firing patterns in the two neurons in Figure 1 resemble the phasic and repetitive firing patterns reported for peripheral sympathetic neurons by others [7, 8, 15]. The possible occurrence of multiple action potentials and the resulting partially summating intracellular Ca^{2+} transients may be crucial for Ca^{2+} dependent signaling systems, and in particular for NFATc movements in SCG neurons (see below). The mean peak amplitude of the peripheral $\Delta F/F_0$ signals in phasic neurons was 0.64 ± 0.24 (in a range from 0.21 to 1.39; n = 30). In repetitively responding neurons, the mean $\Delta F/F_0$ amplitude at the peak of the initial Ca^{2+} transient was 0.57 ± 0.30 (in a range from 0.18 to 1.46; n = 30). The mean $\Delta F/F_0$ at the peak of the first transient in the repetitively firing neurons was not statistically different (at $p < 0.05$) from the peak in phasic neurons. However, due to the partial summation of successive transients, the mean $\Delta F/F_0$ at the highest peak in the repetitively firing neurons was 2.5 ± 0.8 ($p < 0.005$), and the total duration of elevated Ca^{2+} was typically much longer (12 ms time to peak for the single transients, and 245 ms time to final peak for the repetitive transients for the neuron illustrated in Figure 1 B).

In SCG neurons the time course of the Ca^{2+} transients was the same at various AOIs around the cell periphery for each type of firing pattern (phasic, Figure 2 A, or tonic, Figure 2 B). The same pattern of single or repetitive Ca^{2+} signals that appeared at the periphery spread with decrement and time delay into the more centrally located, nonnuclear areas of the cell (Figure 2 A and B, compare traces from AOIs 1, 5 and 9 with those from AOIs 4, 8 and 12). The fluorescence signal from the nucleus was slower and it continued to rise during the decaying phase of the phasic neuron response in the cytosol (Figure 2 A; bottom trace), or during the "plateau" phase of the repetitive cytosolic Ca^{2+} signals in the tonic neuron (Figure 2 B; bottom trace). These observations are consistent with a delayed diffusion of

cytosolic Ca^{2+} into the nucleus. The much longer duration of elevated cytosolic Ca^{2+} in the repetitively responding neuron gave rise to a much larger nuclear Ca^{2+} transient (note the difference in vertical scales in Figures 1 A and 2 A compared to 1 B and 2 B, respectively).

3.2. Electrical and optical recording of repetitive action potential activity and corresponding Ca^{2+} transients

Simultaneous recording of membrane potential and fluo-4 Ca^{2+} transients in perforated patch current clamped SCG neurons revealed that each action potential initiated a corresponding Ca^{2+} transient in both phasic (Figure 2 C) and tonic (Figure 2 D) SCG neurons cultured for 24 hr. The distribution of SCG neurons between the tonic/adapting and phasic behaviors changed systematically with time in culture. In younger cultures (8–24 hrs after plating) repetitive firing dominated (in 40 of 48 neurons evaluated), whereas after 3–5 days phasic behavior became dominant (in 62 of 67 neurons evaluated). Both optical recording (Figure 3 A) and whole cell electrical recording of SGN membrane potential (Figure 3 B) demonstrated the occurrence of the phasic and repetitive firing patterns in our 24 hr cultured SCG neurons. In Figures 3 A and 3 B, representative recordings are illustrated by using either perforated patch current clamp recording and employing a long depolarizing suprathreshold current step, or initiated by a single 2 ms external field stimulus and recorded using the rapidly responding potential sensitive dye annine-6 [16], respectively. Note that in Figures 3 A and B, each panel (a, b and c are from different cells.

Using narrow band scanning (512×30 lines) of annine-6 stained 4 day cultured SCG neurons, which are predominantly phasic, we observed that there was a slow depolarization following the first action potential initiated by a single 2 ms field stimulus (vertical arrow). In some neurons, this slow depolarization initiated subsequent action potentials (Figure 3C; diagonal arrows), whereas in others no subsequent action potentials were produced (not shown). Using longer pulses (10–20ms duration) we found that in some cells the action potential was initiated at the start of the field stimulus, whereas in others the action potential was triggered at the end of the stimulus (data not shown), presumably due to anodal break excitation. Simultaneous recording of optically and electrically recorded membrane potential signals from current clamped SGNs showed good correspondence (Figure 3D).

3.3. Ba^{2+} application increases repetitive firing

Figure 4 presents results from four other SCG neurons. Here a single 2 ms electric field stimulus (arrows) initiated a *train* of partially summating intracellular Ca^{2+} transients under control conditions in one cell, (Figure 4 B, black records from each AOI), but not in another cell (Figure 4 A, black records), even though both cells were from the same 24 hr culture. Application of the K^+ channel blocker Ba^{2+} induced repetitive, partially summating Ca^{2+} transients in the initially non-repetitive neuron (Figure 4 A, red records), and increased the frequency and number of Ca^{2+} transients in the initially repetitively responding neuron (Figure 4 B, red records). Extracellular application of the K^+ channel blocker Ba^{2+} is commonly used to inhibit M-type K^+ currents [17, 18]. In addition, in sympathetic neurons Ba^{2+} has been shown to induce strong SFF [10]. Here we used Ba^{2+} to induce SFF. Accordingly, in 3 day cultured SCG neurons, a stage where phasic firing is dominant, in current-clamp conditions extracellular application of Ba^{2+} (2mM) increased the firing rate (Figure 4C; red trace) of the initially phasic neuron (Figure 4C; black trace), resulting in a pattern similar to that in cells in short time cultures. Figure 4 D shows the inhibitory effect of 2 mM Ba^{2+} on whole-cell M-type K^+ currents in a 2-day old cultured SCG neuron. The almost complete inhibition of the M-type current by this concentration of Ba^{2+} confirms that the firing frequency of sympathetic neurons is critically dependent on the level of M-type K^+ conductance [7, 8, 10]. Interestingly, the repetitive firing rate in the SCG neurons is about 5–20 Hz (Figures 1–3), generally similar to the 10 Hz effective frequency for NFAT

translocation observed previously in experiments on skeletal muscle [14] and here in SCG neurons (below).

3.4. Ca^{2+} transients during 1 and 10 Hz train stimulation

SCG neurons in 3–5 day cultures exhibited predominantly phasic firing patterns in response to single stimuli under control conditions (Figures 5 A and B, traces from two different neurons). However, stimulation of such neurons with a 5 s duration train of repetitive stimuli at 1 Hz gave rise to repeated fluo-4 Ca^{2+} transients at 1 s intervals (Figure 5 C). These repeated fluorescence signals exhibited similar time courses and similar slight extents of summation at various AOIs around the non-nuclear cell periphery during the 1 Hz train of stimuli, whereas the fluorescence signals from the peripherally located nucleus exhibited a somewhat greater extent of summation than the peripheral cytoplasmic regions (Figure 5 C). In contrast, during a 5 s interval of 10 Hz train stimulation, the extent of Ca^{2+} transient summation was considerably greater in both the peripheral cytoplasm and the nucleus (Figure 5 D; same neuron as in Figure 5 B) than during 5 s of stimulation at 1 Hz. During the 45 s intervals between the repeated 5 s trains of stimuli at 10 Hz the fluo-4 fluorescence signal returned to near base line level (data not shown).

3.5. Expressed NFATc1-CFP translocates from cytoplasm to nucleus in rat SCG neurons during prolonged depolarization or kinase inhibition

48 hr after infection of 2-day cultures of rat SCG neurons with the adenovirus NFATc1-CFP, the CFP fluorescence was present predominantly in the cell cytoplasm, with little fluorescence in the nucleus under control conditions (Figure 6 A,a and B,b). Tonic depolarization with elevated KCl (50 mM, 20–60 min) caused nuclear translocation and decreased cytosolic NFATc1-CFP fluorescence in cultured SCG neurons (Figure 6 A,a'), as previously observed by others in hippocampal neuron cultures [4]. Block of phosphorylation activity with the non-specific kinase inhibitor staurosporin (5 μM, 20–60 min) also resulted in translocation of NFATc1-CFP from the cytoplasm to the nucleus in SCG neurons (Figure 6 B,b'). This indicates that a dynamic equilibrium exists between NFAT dephosphorylation and phosphorylation in unstimulated cultured neurons, and that block of phosphorylation (by staurosporin) shifts the balance to dephosphorylation and consequent NFAT entry into the nucleus. As a negative control, expressed CFP (i.e., with no NFAT moiety) was present in both the cytosol and the nucleus (Figure 6 C,c'), and did not change its intracellular distribution during the same stimuli (data not shown). Note that CFP itself is small enough to pass through the nuclear pore, whereas NFAT-CFP is too large and requires importin-dependent nuclear import mediated by the NFAT nuclear localization signal (NLS), which is masked in phosphorylated NFAT and is unmasked by NFAT dephosphorylation [3]. Using RT-PCR analysis, we found that NFATc1, as well as the other Ca^{2+} - sensitive NFAT isoforms (c2–c4) are all expressed at the mRNA level in rat SGNs (Figure 6 D).

3.6. Relationship between action potential patterns and NFATc1 nuclear translocation

Repetitive, partially summating Ca^{2+} transients, such as those in Figure 1B, Figure 2B and Figure 4B, may initiate cellular responses that would not be induced by single isolated Ca^{2+} signals [19]. We used NFATc1-CFP to examine this possibility. In resting cells NFATc1 is phosphorylated and located in the cytosol. Elevated cytosolic Ca^{2+} activates the Ca^{2+} sensitive phosphatase calcineurin, resulting in NFAT dephosphorylation, which leads to the exposure of the NFAT nuclear localization signal, followed by nuclear entry of dephopshorylated NFAT [2, 3]. 40 min of repetitive field stimulation with 5 s trains of stimuli at 1 Hz once every 50 s caused negligible translocation of NFATc1-CFP into SGN nuclei in 5 day culture (Figure 7A and B, top). However when the same stimulation protocol was applied in the presence of 2 mM Ba^{2+}, which induced repetitive action potentials and corresponding Ca^{2+} transients in other SCG neurons, a significant nuclear translocation of

NFATc1 (Figure 7A and B, bottom) was observed, consistent with greater activation of calcineurin due to the additional Ca^{2+} transients initiated by the presence of Ba^{2+} (Figure 4). In all cases, 20–60 min application of the non specific kinase inhibitor staurosporin (5 μM) after the tests in Figure 7A and B resulted in further increase in nuclear NFATc1 (Figure 7C and D), indicating that block of phosphorylation (by staurosporin) shifts the dynamic balance between phosphorylation and dephosphorylation to dephosphorylation, resulting in NFAT entry into the nuclei. Thus, NFATc1 was mobile even in cells that were stimulated at 1 Hz and exhibited no stimulation-dependent nuclear translocation after stimulation for 40 min at 1 Hz (Figure 7, top).

40 min of repetitive application of 5 s trains of stimuli at 10 Hz once every 50 s in the absence of Ba^{2+} also produced significant nuclear translocation (Figure 8A), consistent with greater activation of calcineurin compared to that produced by 1 Hz stimulation, due to the larger number and summation of Ca^{2+} transients during 10 Hz stimuli (Figure 5). The 10 Hz train stimulation pattern induced significant nuclear translocation of NFATc1 ($P< 0.0007$; $N = 18$, see Figure 8 A), whereas 1 Hz train did not ($P = 0.41$; $N = 28$, see Figure 7 A and B, top). However, 1 Hz train stimulation did result in significant NFATc1 translocation in the presence of 2 mM Ba^{2+} ($P<0.0022$; $N = 34$, see Figure 7 A and B, bottom), which promotes repetitive firing and the accompanying repetitive, partially summating Ca^{2+} transients.

3.7. N-type Ca^{2+} channels as main source of Ca^{2+} influx for Ca^{2+} transient initiation and NFATc1 translocation in cultured rat SCG neurons

The Ca^{2+} current in cultured SCG neurons is carried ~65–90% by N-type channels, with the remainder carried by L- and R-type channels, with negligible P/Q component [11, 20]. NFATc1 nuclear translocation during 10 Hz train stimulation was insensitive to the L-type Ca^{2+} channel blocker nifedipine (5 μM; Figure 8B), but was completely suppressed by 1.3 μM of the specific N-type Ca^{2+} channel blocker ω-conotoxin-GVIA in 5 day cultured SGNs. (Figure 8C). We also measured whole-cell Ca^{2+} current density using 5 mM calcium as the charge carrier. A test depolarization to −10 mV from a holding potential of −80 mV elicited inward Ca^{2+} currents of ~30 pA/pF (Figure 8D). The addition of ω-conotoxin-GVIA to the extracellular solution blocked ~80 % of the whole-cell Ca^{2+} current of 2–5 day cultured voltage-clamped SCG neurons (Figure 8D and E). We estimated the contribution of N-type calcium current after 3–5 days in culture to be approximately 23 pA/pF, using the ω-conotoxin-GVIA test (Figure 8E). Figure 8F shows that 1.3 μM ω-conotoxin-GVIA almost completely eliminated the AP-induced Ca^{2+} transient elicited by single 2ms field stimulus in four AOIs around the periphery of the neuron. These results suggest that N-type Ca^{2+} channels may provide the majority of the Ca^{2+} influx and be responsible for initiating the Ca^{2+} transient in cultured SCG neurons. In another set of neurons, we applied 5 μM nifedipine, an L-type Ca^{2+} channel blocker, and found that it had little or no effect on AP-induced Ca^{2+} transients (data not shown). These findings further confirm that N-type Ca^{2+} channels provide the main Ca^{2+} influx pathway for initiating Ca^{2+} transients in cultured SCG neurons.

3.8 Time course of NFATc1 nuclear entry during repetitive trains of electric field stimulation

Figure 9 A and B show that under control conditions, in the absence of electrical stimulation, the nucleo-cytoplasmic distribution of NFATc1-CFP was stable over time. However, within 10 min of the start of repetitive electrical field stimulation with 5 s trains of 10 Hz stimuli delivered once every 50 s, there was a clear increase in nuclear NFATc1-CFP fluorescence, and a corresponding drop in cytosolic NFATc1-CFP fluorescence, consistent with a redistribution of NFATc1 from cytosol to nucleus. This redistribution continued during about the first 20 min of repetitive 10 Hz train stimulation, and then reached an

apparent steady distribution despite continued repetitive stimulation for another 20 min (Figure 9 A and B). In contrast, a similar stimulation protocol, but now using 5 s trains of 1 Hz stimuli, which give much smaller summated Ca^{2+} transients (see Figure 5), produced little if any translocation of NFATc1-CFP from cytoplasm to nucleus (Fig 9 C and D), consistent with much less activation of calcineurin for the smaller Ca^{2+} transients for the 1 Hz trains compared to the 10 Hz trains.

4. Discussion

Here we have used high speed confocal imaging to monitor the spatio-temporal pattern of spread of elevated Ca^{2+} in 1 day cultured rat SCG neurons exhibiting either single or multiple action potentials in response to a single field stimulus. We find that the Ca^{2+} transient is similar around the cell periphery and spreads into the cell in each type of cell, with the repetitively firing cells exhibiting summation and longer overall duration of the Ca^{2+} signals than the phasic neurons. Using 3–5 day cultured SCG neurons, which under control conditions exhibit only a single action potential in response to each field stimulus, we found that NFATc1-CFP exhibited brisk translocation from cytoplasm to nuclei during repetitive stimulation using a 5 s duration train of 10 Hz electric field stimuli applied once every 50 s. In contrast, repeated 5 s duration trains of 1 Hz stimuli, also applied once every 50 s, did not cause detectable NFATc1-GFP nuclear translocation under control conditions. However, when the same repetitive 1 Hz train stimulation pattern was applied in the presence of Ba^{2+}, which induces repetitive firing at about 5–20 Hz, likely by inhibiting M-type K^+ channels, and thereby produces repeated summating Ca^{2+} transients at the same frequency, we did observe major NFATc1-CFP nuclear translocation. Thus, repetitive 5 s trains of summating Ca^{2+} transients at 5–20 Hz given once every 50 s provide a sufficient degree of calcineurin activation and consequent NFAT dephosphorylation during the train for a majority of the cytosolic NFATc1-CFP to move from cytoplasm to nucleus in SCG neurons, and to remain in the nucleus in a steady state during continuation of the repeated trains of stimuli and corresponding Ca^{2+} transients. During the steady state, the net NFAT entry into the nucleus during each train is presumably balanced by an equal amount of NFAT efflux from the nucleus between the trains. Our primary conclusion is that both the frequency of external stimulation and the intrinsic ionic mechanisms determining the resulting action potential and Ca^{2+} transient pattern(s) strongly affect the degree of NFATc activation and nuclear translocation.

Ca^{2+} transient and stimulation patterns dependent NFATc1 nuclear translocation in SCG neurons and skeletal muscle fibers

In skeletal muscle fibers isolated from mouse *flexor digitorum brevis* muscles, we previously found that the same pattern of 5 s trains of 10 Hz stimuli delivered once every 50 s also produced NFATc1-GFP nuclear translocation, whereas even continuous stimulation at 1 Hz was ineffective in producing nuclear translocation [14]. However, there are a number of differences between these two systems. In skeletal muscle fibers, the fluo-4 signals for 10 Hz trains are considerably larger and faster than the fluo-4 signals recorded here for 10 Hz trains in SCG neurons. In muscle, the fluo-4 Ca^{2+} signal rises to several fold times the resting value in response to each pulse in the 10 Hz train, but then declines to about twice the resting fluorescence just before the next pulse in the train [21]. In contrast, in the SCG neurons, the fluo-4 signals for each pulse are much smaller than in muscle fibers. However, near the start of the 10 Hz train, the transients exhibit relatively little decline by the time of the next pulse, causing a continuous build up of Ca^{2+}, which reaches a steady state of about twice the resting value before the end of the 5 s train of 10 Hz stimuli in the SCG neurons. Thus, the time integral of elevated Ca^{2+} during the trains of 10 Hz stimuli, which may

determine the extent of activation of calcineurin in each system, may not be that dissimilar in the SCG neurons studied here and in the skeletal muscle fibers studied previously.

Enhancement of repetitive action potentials, Ca^{2+} signals and NFATc translocation

In the conditions used to evaluate NFATc translocation in 3–5 day cultured neurons, most of the neurons displayed phasic behavior in response to a suprathreshold stimulus (Figure 4 C), likely the result of M-channel current activity and SFA, and extracellular application of Ba^{2+} resulted in an increase in the number of action potentials. Several lines of evidence suggest that Ba^{2+} might act mainly by inhibiting M-channels (see Figure 4 D [17, 18]). The important role of the M-current in controlling membrane excitability and thereby mediating or inhibiting such repetitive firing has been demonstrated [7; 22, 23, reviewed in 8]. Furthermore, in cultured sympathetic neurons, Ba^{2+} has been shown to induce M-current inhibition and strong SFF [10]. Our results with Ba^{2+} support the important role of M-current inhibition during SFF, thus implicating M-channels as key elements during low frequency-dependent NFATc activation. However, additional effects of Ba^{2+} on other K^+ channels cannot be excluded. Other physiological mechanisms that may potentially produce or enhance SFF include inhibition of AHP-type currents, mediated by Ca^{2+}-dependent K^+ channels, fast recovery from inactivation of the fast sodium channel, resurgent sodium current, and synaptic facilitation [9, 24].

In hippocampal neurons, L-type voltage dependent Ca^{2+} channels have been shown to mediate Ca^{2+} influx to activate NFATc4 translocation [4]. It also has been shown that the majority of the Ca^{2+} current in cultured peripheral sympathetic neurons flows through N-type Ca^{2+} channels, with the remainder carried by L- and R-type Ca^{2+} channels and negligible detectable P/Q component [11, 20]. Our results on Figure 8 confirmed this. Thus, N-type Ca^{2+} channels act as a main source of Ca^{2+} influx to activate NFATc in these neurons. The contribution of intracellular Ca^{2+} sources, in particular, the extent to which the Ca^{2+} influx is amplified by Ca^{2+} release from intracellular stores due to Ca^{2+} induced Ca^{2+} release [1, 25] remains to be determined. Nonetheless, N-type Ca^{2+} channels clearly provide the main source of Ca^{2+} influx for initiating the Ca^{2+} transients leading to activation of NFATc in these neurons.

Repetitive action potential firing and single brief electrical field stimulation

The firing behavior of intact and adult rat SCG neurons, based on their response to constant depolarizing current step, has been classified as exclusively ‘phasic’ [22, 23]. Here, unexpectedly, we found that in 8–48 hr cultured rat SCG neurons a long depolarizing current step revealed both phasically and tonically firing neurons. After 3–7 day in culture, almost all the neurons displayed a phasic firing during a constant current depolarization.

In peripheral sympathetic neurons, M-channel current density constitutes a key element in mediating phasically or tonically firing behavior [7, 8, 22, 23]. Thus, one possible explanation to the occurrence of tonically firing neurons between 8–48 hr after plating might be a reduction on M-current density, likely because of the mechanic and enzymatic dissociation procedure and the resulting lost of neuronal prolongations. The eventual outgrowth of neuronal processes and the recovery of M-channel current density that occur in 3–5 day cultured SCG neurons might explain the re-establishment of the phasic behavior (unpublished observations; see Fig 1 in [10]).

In 1 day cultured neurons, or during Ba^{2+} application in neurons cultured for 2–4 days, a single 2 ms field stimulus was able to induce multiple APs and the corresponding partially summating Ca^{2+} transients. One possible explanation to the occurrence multiple action potentials during single field stimulation is provided by the transient and reversible

formation of microscopic conductive pores [*reversible electroporation*; 26, 27]. These pores would allow ionic influx from the external medium that is robust enough to induce partial membrane depolarization until the plasma membrane is re-sealed [26]. In this case, a single field stimulus could behave effectively as a current pulse followed by a slowly decaying current. It is important to mention that we found that electrical stimuli applied in this study did not induce the formation of 'irreversible' or long-lasting pores [irreversible electroporation], as indicated by cellular exclusion of extracellularly applied propidium iodide or fluo-4 (data not shown), and by the reproducibility of the neuron's responses from trial to trial. An alternative possible mechanism to explain the repetitive AP firing observed here in response to 1 ms field stimuli could be the spontaneous oscillatory firing mechanism mediated by the resurgent sodium current described in other neuronal types [24].

NFAT activation and functional consequences

In adult hippocampal neurons, activation of NFATc4 has been demonstrated during spontaneous and induced electrical activity [4], as well as during neurotrophin-induced transcription [28]; its activation was proposed to be crucial in the induction of synaptic plasticity and memory formation. In spinal neurons, neurokinin receptor activation by substance P resulted in NFATc4 activation [29]; its activation was proposed to occur during peripheral tissue injury and to play a role in chronic pain. Neuronal survival [5], axonal outgrowth stimulation [30] and axon terminal remodeling [6] correlated tightly with the nuclear activation of NFATc. Hence, NFATc-mediated gene expression has been proposed as a key step during neuronal morphogenesis and development, synaptic plasticity and neuronal function. In rat SCG neurons, the specific group of genes regulated after NFAT activation, as well as their functional consequences, are still under examination.

In sympathetic ganglia, preganglionic axons form synapses with somatodendritic membranes of postganglionic neurons, and release acetylcholine and other transmitters and neuropeptides [31]. Phasic neurons predominate in sympathetic ganglia and are characterized by the presence of M channels [22, 23, reviewed in 31], which in turn are regulated by many transmitters and drugs including linopirdine, a cognition enhancer in animal models [32], and imipramine, an antidepressant [33]. Thus, transmitters and neuropeptides released from preganglionic axons, as well as some therapeutic drugs may be important in maintaining and/or adapting sympatho-effector transmission by regulating M-channels. In turn, M-channel activity will affect action potential firing patterns and gene expression via Ca^{2+} dependent regulation by NFAT or other activity-driven transcriptional factors.

Finally, the importance of the temporal pattern and frequency of Ca^{2+} transients on NFATc-mediated gene expression has been previously demonstrated in lymphocytes and muscle fibers [14, 19]. Specific Ca^{2+}/frequency-dependent transcription factor activation seems to be present in numerous cell types, including SCG neurons, and may constitute a code that underlies plastic changes occurring over minutes, hours or days in these cells.

Acknowledgments

The authors wish to thank Ms. Carrie Wagner for technical assistance, Mr. Gabe Sinclaire and Mr. Jeff Michael for design and construction of custom mechanical and electronic apparatus, Drs William Randall and Yewei Liu for developing and providing the NFATc1-CFP adenovirus used in these studies, and Dr Daniel Weinreich for comments on this work. Supported by NIH Grant R01-NS042839.

References

1. Berridge MJ. Neuronal calcium signaling. Neuron. 1998; 21:13–26. [PubMed: 9697848]

2. Beals CR, Clipstone NA, Ho SN, Crabtree GR. Nuclear localization of NF-ATc by a calcineurin-dependent, cyclosporine-sensitive interaction. Genes Dev. 1997; 11:824–834. [PubMed: 9106655]
3. Rao A, Luo C, Hogan PG. Transciption factors of the NFAT family: regulation and function. Annu. Rev. Immunol. 1997; 15:707–747. [PubMed: 9143705]
4. Graef IA, Mermelstein P, Stankunas K, Neilson J, Deisseroth P, Tsien RW, Crabtree G. L-type calcium channels and GSK-3 regulate the activity of NF-ATc4 in hippocampal neurons. Nature. 1999; 401:703–708. [PubMed: 10537109]
5. Benedito AB, Lehtinen M, Massol R, Lopes U, Kirchhausens T, Rao A, Bonni A. The Transcription Factor NFAT3 Mediates Neuronal Survival. J. Biol. Chem. 2005; 280:2818–2825. [PubMed: 15537643]
6. Yoshida T, Mishima N. Distinct roles of calcineurin–nuclear factor of activated T cells and protein kinase A-cAMP response element-Binding protein signaling in presynaptic differentiation. J. Neurosci. 2005; 25:3067–3079. [PubMed: 15788763]
7. Brown DA, Adams PR. Muscarinic suppression of a novel voltage-sensitive K^+ current in a vertebrate neurone. Nature. 1980; 283:673–676. [PubMed: 6965523]
8. Delmas P, Brown DA. Pathways modulating neural KCNQ/M (Kv7) potassium channels. Nat. Rev. Neurosci. 2006; 6:850–862. [PubMed: 16261179]
9. Benda J, Herz AV. A universal model for spike-frequency adaptation. Neural Comput. 2003; 5:2523–2564. [PubMed: 14577853]
10. Romero M, Reboreda A, Sanchez E, Lamas JA. Newly developed blockers of the M-current do not reduce spike frequency adaptation in cultured mouse sympathetic neurons. Eur. J. Neurosci. 2004; 19:2693–2702. [PubMed: 15147303]
11. Garcia-Ferreiro RE, Hernandez-Ochoa EO, Garcia DE. Modulation of N-type Ca^{2+} channel current kinetics by PMA in rat sympathetic neurons. Pflugers Arch. 2001; 442:848–858. [PubMed: 11680617]
12. Hamill OP, Marty A, Neher E, Sakmann B, Sigworth FJ. Improved patch-clamp techniques for high-resolution current recording from cells and cell-free membrane patches. Pflugers Arch. 1981; 391:85–100. [PubMed: 6270629]
13. Horn R, Marty A. Muscarinic activation of ionic currents measured by a new whole-cell recording method. J. Gen. Physiol. 1988; 92:145–159. [PubMed: 2459299]
14. Liu Y, Cseresnyes Z, Randall WR, Schneider MF. Activity-dependent nuclear translocation and intranuclear distribution of NFATc in adult skeletal muscle fibers. J. Cell Biol. 2001; 155:27–39. [PubMed: 11581284]
15. Malin SA, Nerbonne JM. Elimination of the fast transient in superior cervical ganglion neurons with expression of KV4.2W362F: Molecular Dissection of I_A. J. Neurosci. 2000; 20:5191–5193. [PubMed: 10884302]
16. Kuhn B, Fromherz P, Denk W. High sensitivity of Stark-shift voltage-sensing dyes by one- or two-photon excitation near the red spectral edge. Biophys. J. 2004; 87:631–639. [PubMed: 15240496]
17. Constanti A, Adams PR, Brown DA. Why do barium ions imitate acetylcholine? Brain Res. 1981; 206:244–250. [PubMed: 6970607]
18. Brown DA, Selyanko AA. Membrane currents underlying the cholinergic slow excitatory post-synaptic potential in the rat sympathetic ganglion. J. Physiol. 1985; 365:365–387. [PubMed: 2411921]
19. Dolmetsch RE, Xu K, Lewis RS. Calcium oscillations increase the efficiency and specificity of gene expression. Nature. 1998; 392:933–936. [PubMed: 9582075]
20. Plummer MR, Logothetis DE, Hess P. Elementary properties and pharmacological sensitivities of calcium channels in mammalian peripheral neurons. Neuron. 1989; 2:1453–1463. [PubMed: 2560643]
21. Liu Y, Randall WR, Schneider MF. Activity-dependent and -independent nuclear fluxes of HDAC4 mediated by different kinases in adult skeletal muscle. J. Cell. Biol. 2005; 168:887–897. [PubMed: 15767461]
22. Brown DA, Constanti A. Intracellular observations on the effects of muscarinic agonists on rat sympathetic neurons. Br. J. Pharmacol. 1980; 70:593–608. [PubMed: 7470731]

23. Wang H, McKinnon D. Potassium currents in rat prevertebral and paravertebral sympathetic neurons: control of firing properties. J. Physiol. 1995; 485:319–335. [PubMed: 7666361]
24. Raman IM, Bean BP. Resurgent sodium current and action potential formation in dissociated cerebellar Purkinje neurons. J. Neurosci. 1997; 17:4517–4526. [PubMed: 9169512]
25. Verkhratsky A. Physiology and pathophysiology of the calcium store in the endoplasmic reticulum of Neurons. Physiol. Rev. 2005; 85:201–279. [PubMed: 15618481]
26. Bier M, Chen W, Gowrishankar TR, Astumian RD, Lee RC. Resealing dynamics of a cell membrane after electroporation. Phys. Rev. E. Stat. Nonlin. Soft Matter Phys. 2002; 66 062905.
27. DeBruin KA, Krassowska W. Modeling electroporation in a single cell. I) Effects of field strength and rest potential. Biophys. J. 1999; 77:1213–1224. [PubMed: 10465736]
28. Groth R, Mermelstein P. Brain-Derived Neutrophic Factor Activation of NFAT (Nuclear Factor of Activated T-Cells)-Dependent Transcription: A role for the Transcription Factor NFATc4 in Neurotrophin-Mediated Gene Expression. J. Neurosci. 2003; 23:8125–8134. [PubMed: 12954875]
29. Seybold VS, Coicou LG, Groth RD, Mermelstein PG. Substance P initiates NFAT-dependent gene expression in spinal neurons. J. Neurochem. 2006; 97:397–407. [PubMed: 16539671]
30. Graef IA, Wang F, Charron F, Chen L, Neilson J, Tessier-Lavigne M, Crabtree GR. Neurotrophins and netrins require calcineurin/NFAT signaling to stimulate outgrowth of embryonic axons. Cell. 2003; 113:657–670. [PubMed: 12787506]
31. Boehm S, Kubista H. Fine tuning of sympathetic transmitter release via ionotropic and metabotropic presynaptic receptors. Pharmacol. Rev. 2002; 54:43–99. [PubMed: 11870260]
32. Lamas JA, Selyanko AA, Brown DA. Effects of a cognition-enhancer, linopirdine (DuP 996), on M-type potassium currents (IK(M)) and some other voltage- and ligand-gated membrane currents in rat sympathetic neurons. Eur. J. Neurosci. 1997; 9:605–616. [PubMed: 9104602]
33. Quintero JL, Arenas MI, Garcia DE DE. The antidepressant imipramine inhibits M current by activating a phosphatidylinositol 4,5-bisphosphate (PIP2)-dependent pathway in rat sympathetic neurons. Br. J. Pharmacol. 2005; 145:837–843. [PubMed: 15852030]

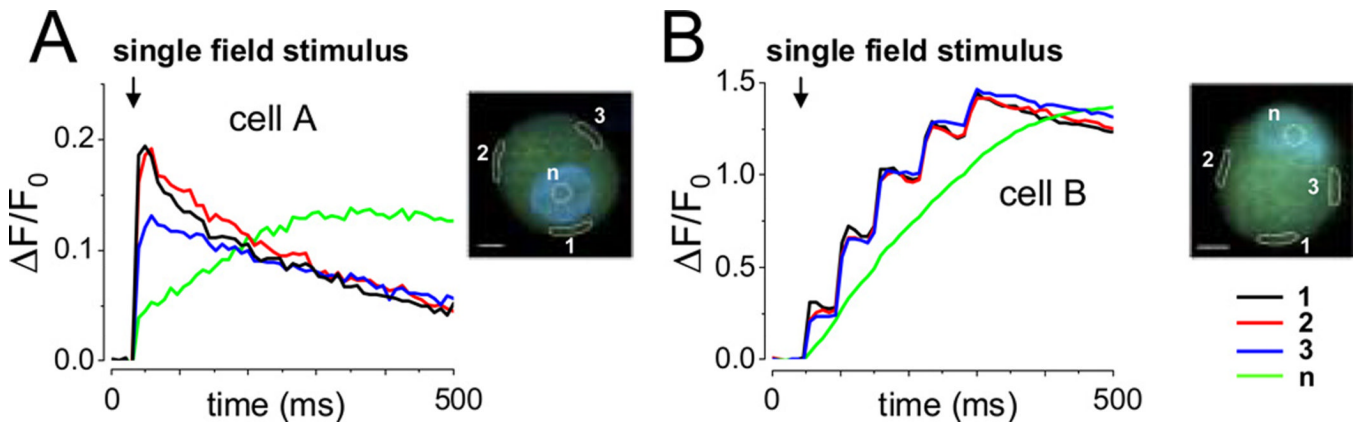

Figure 1.

Temporal properties of local Ca^{2+} signals in neurons during phasic or repetitive firing. Series of successive x–y confocal fluorescence images were recorded at high speed (9.25 ms/frame) in cultured rat SCG neurons, loaded with fluo-4 AM and field stimulated to elicit Ca^{2+} transients. (A–B) Time courses of $\Delta F/F_0$ signals at non-nuclear and nuclear areas of interest (AOIs; indicated as white-colored zones) in two representative neurons showing a single or multiple Ca^{2+} transients in response to a single, 2 ms field stimulus (arrows). DAPI, a DNA dye was used to identify the nucleus more precisely. Scale bar 5 μm.

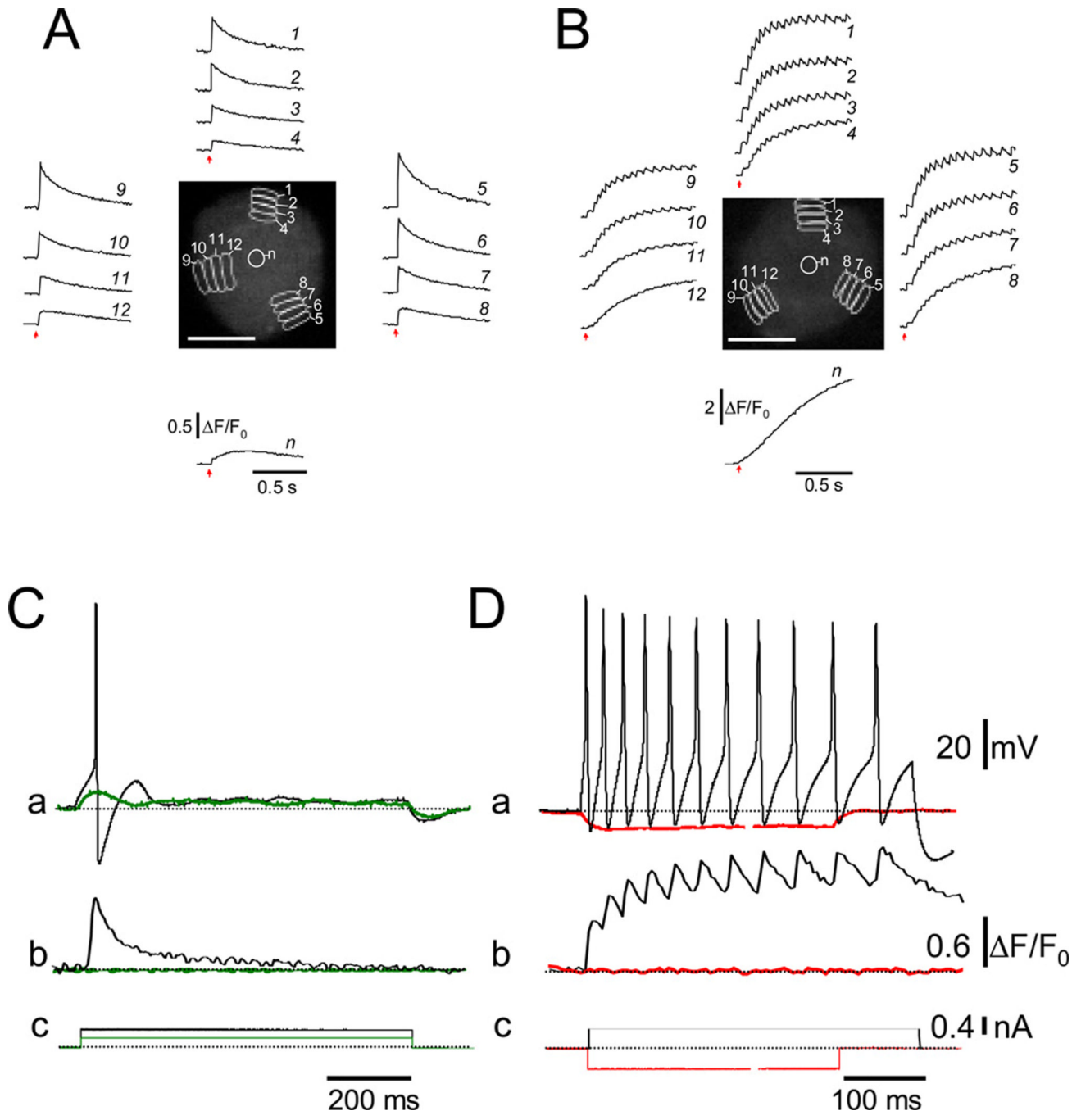

Figure 2.

Radial spread of single (A) and repetitive Ca^{2+} transients (B) in SCG neurons after single 2 ms field stimulation (arrows). Three AOIs at the cell periphery (AOIs 1, 5 and 9 in panels A and B), together with three radially shifted AOIs each, were selected and the $\Delta F/F_0$ values were calculated. The time course of $\Delta F/F_0$ at a nuclear AOI (n) was plotted at the bottom of the central panel for each neuron. Action potential-induced Ca^{2+} transients were observed in phasic (C) and repetitively firing neurons (D). Membrane potential changes (perforated patch; upper traces) and fluo-4 Ca^{2+} signals (middle traces) were recorded simultaneously in two 24h cultured SCG neurons. Dashed lines mark the resting potential (−60 mV). Red traces show membrane potential measurements and fluo-4 signals in response to

subthreshold stimuli. Black traces show single (C) or multiple action potentials (D) in response to suprathreshold current pulses, in phasic and repetitive firing neurons, respectively. Note that each action potential was followed by a Ca^{2+} transient. The gap in the red records in panel Da and Dc corresponds to 250–750 ms. Scale bar 10 μm.

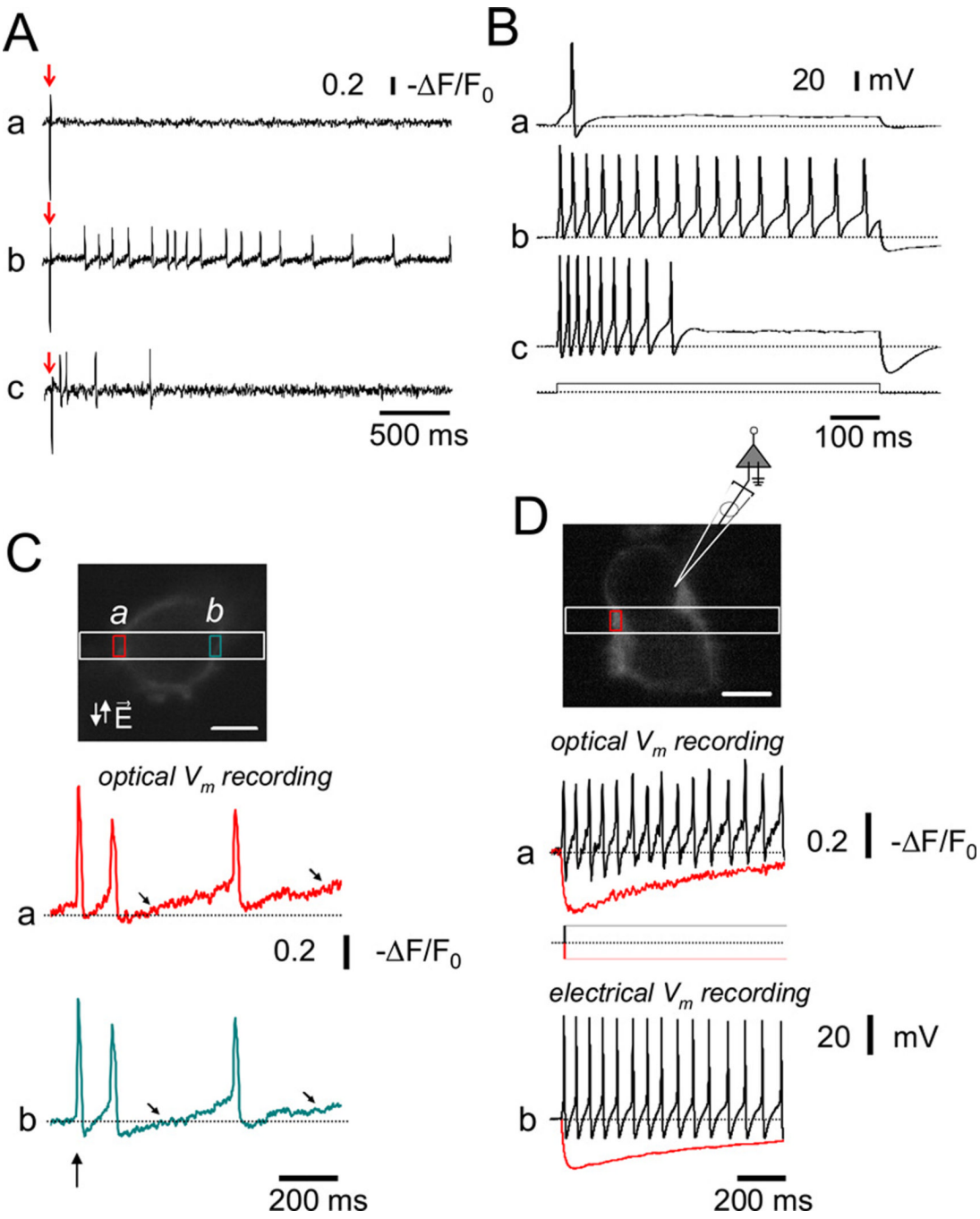

Figure 3.

Phasic and repetitive firing patterns in 24 hr cultured rat SCG neurons. (A) Representative action potential recordings from phasic (a), and repetitively firing neurons (b–c) using annine-6, a fast response voltage-sensitive dye (see Material and Methods). In each neuron, action potentials were elicited by single 2ms suprathreshold field stimuli (indicated by arrows). (B) Action potentials in response to long (800 ms) suprathreshold depolarizing current steps (400 pA) were recorded in current-clamp mode from three 24 hr cultured SCG neurons (Figure 3B a–c). Based on the response(s) to these current injections, neurons were classified as either phasic (a), or repetitively firing (b and c). After 24 hr in culture, ~48 % of the SCG neurons responded with a single AP or displayed phasic firing (i.e. firing up to 3

action potentials in response to long, suprathreshold current injections). Repetitive firing was observed in the remaining ~52 % of the neurons evaluated in this study (n = 48). (C) Top. Fluorescence of an annine-6 stained 4 day cultures SCG neuron scanned in *x–y* mode. A band scan (512× 30 lines; 723 fps; 1.3 ms per frame) was acquired at the region enclosed by the white rectangle. During the band scan a single 2 ms field stimulus (vertical arrow) was applied and the time course of the fluorescence (a) and (b) was evaluated at the plasma membrane in two AOI's (a and b, red and cyan boxes on *xy* image, respectively). A slow depolarization (diagonal arrows) followed the first action potential initiated by a single 2 ms field stimulus (vertical arrows). (D) Simultaneous recording of optically and electrically measured membrane potential signals from an annine-6 stained and current-clamped SCG neuron. Top. Fluorescence of a different annine-6 stained and voltage-clamped SCG neuron scanned in *x–y* mode. The cartoon illustrates the position of the patch pipette and the AOI (red box) used for the evaluation of the time course (a) of annine-6 fluorescence during either negative (red trace) or positive (black trace) current steps. (b) Membrane potentials measurements acquired with the current protocol illustrated at the middle of the panels. Note the agreement between the optically and electrically recorded membrane potentials.

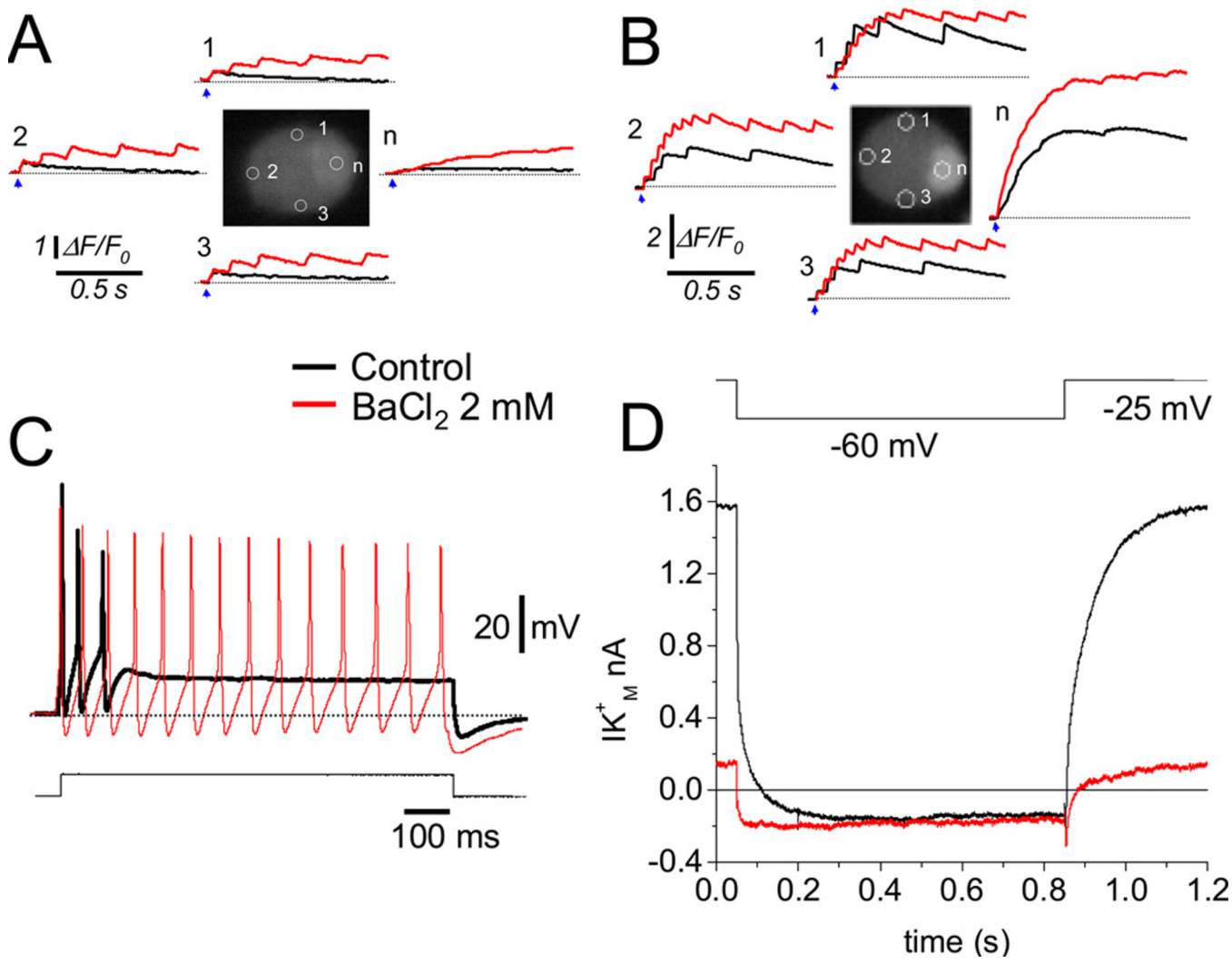

Figure 4.

Extracellular application of Ba^{2+} promotes spike frequency facilitation in cultured SCG neurons. (A) Application of Ba^{2+} (red traces) increased the number of Ca^{2+} transients in an initially phasic neuron (black traces). (B) Addition of Ba^{2+} in an initially repetitively firing neuron increased the number of Ca^{2+} transients. The blue arrows indicate the application of 2 ms field stimulus. Neurons in panels A and B were evaluated 24 hr after plating. (C) Application of Ba^{2+} induced SFF in a 3 day cultured and current-clamped SCG neuron, same cell shown before and after $BaCl_2$ application. After 3 days in culture, ~92% of the SCG neurons displayed phasic firing. Repetitive firing was observed in the remaining ~8 % of the neurons evaluated (n = 67). (D) Inhibition of the M-type K^+ current by 2 mM Ba^{2+}. I_M was activated by setting the holding potential at −25 mV and deactivated by 800 ms command pulses from −25 to −60 mV every 4 s.

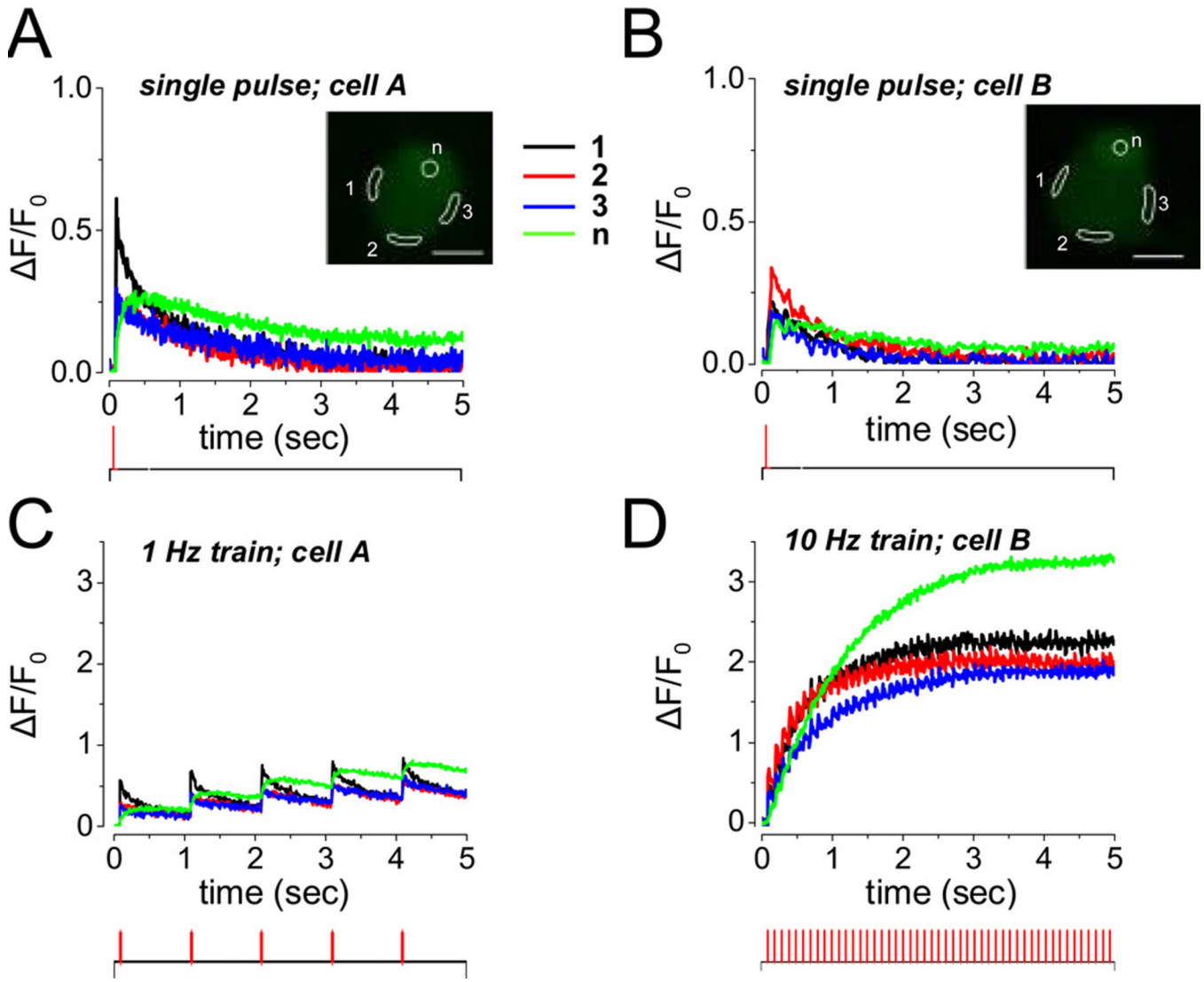

Figure 5.

Fluo-4 fluorescence signals for single stimuli or for 5 s trains of 1 or 10 Hz repetitive electric field stimuli in two 5 day cultured SCG neurons. (A–B) Single stimuli–induced, relatively rapidly rising and falling fluo-4 fluorescence transients in different peripheral AOIs (black, blue and red records), and somewhat slower fluorescence signals in the peripherally located nuclei (green). (A) and (B) recorded from two different neurons. (C) A 5 s train of repeated stimuli at 1 Hz gave partial summation of the fluo-4 fluorescence signals from peripheral cytoplasm and nuclei. (D) A 5 s train of repetitive stimuli at *10 Hz* produced greater summation of the fluorescence signals in both cytoplasm and nuclei. A and C from one neuron, B and D from another neuron. Field stimulation protocols are illustrated at the bottom of each panel.

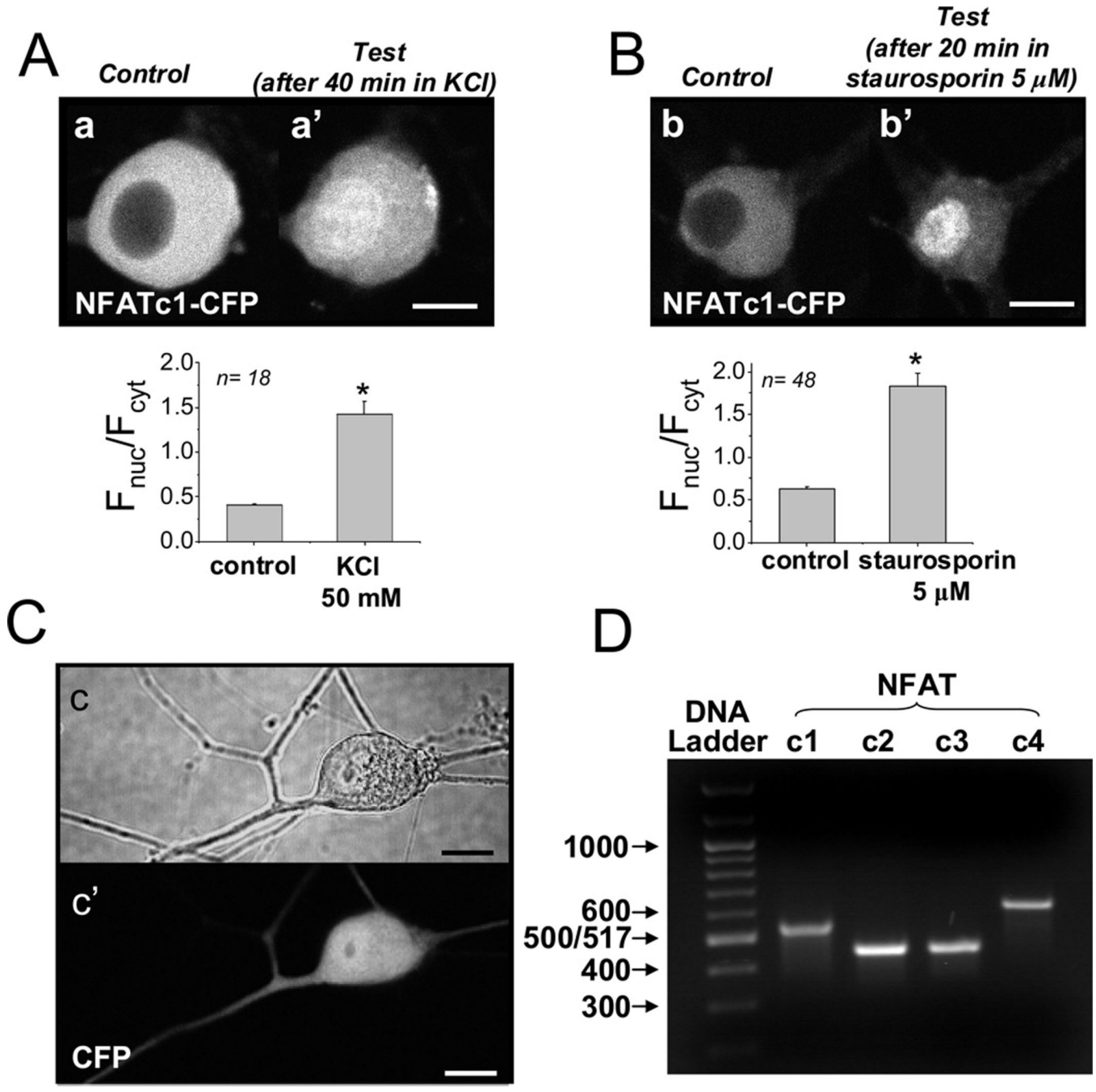

Figure 6.

NFATc1-CFP nuclear translocation induced by tonic depolarization or by inhibition of protein kinases. (A–B) Representative images of 4-day cultured SCG neurons overexpressing NFATc1-CFP before (A, a, and B, b), and after 40 min of tonic depolarization using 50 mM KCl (A, a'), or after 40 min application of staurosporin (5 μM; B, b'). Bar plots, nuclear/cytoplasmic ratios (F_{nuc}/F_{cyt}) for each condition. (C) Representative image of an SCG neuron overexpressing CFP. Note that the expressed CFP (i.e., with no NFAT moiety) was present in both the cytosol and the nucleus, and did not change its intracellular distribution during the same stimuli (data not shown). Scale bars 10

μm. (D) Gel of RT-PCR products obtained using primers for NFAT c1-c4, as indicated. All isoforms are present at the mRNA level in RNA samples extracted from intact rat SCGs.

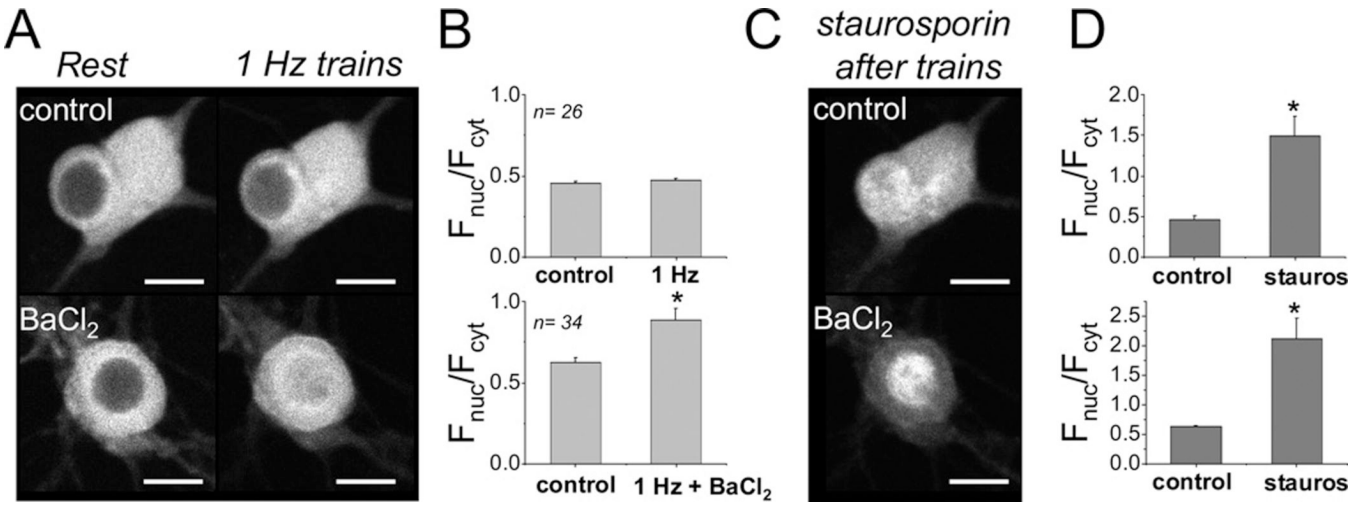

Figure 7.

5 s trains of 1 Hz electrical field stimulation in the presence of $BaCl_2$ successfully induce NFATc1-CFP translocation from cytosol to nucleus. (A–B) Representative images of neurons expressing NFATc1-CFP before (left), and 40 min after the start of electrical stimulation (right) using repetitive application (once every 50 s) of a 5 s 1Hz train in control conditions (top) or after the application of 2 mM Ba^{2+} (bottom). (C–D) 20–60 min application of staurosporin (5 μM) following the test condition in Figure 7A and B resulted in further increase in nuclear NFATc1. Scale bar 10 μm. Images from one respresentative neuron are shown in the top row of A and C, and from another neuron in the bottom row in A and C. n = 26 for the top row of B and D, and 34 for the bottom row of B and D. Bar plots, nuclear/cytoplasmic ratios (F_{nuc}/F_{cyt}) for each condition.

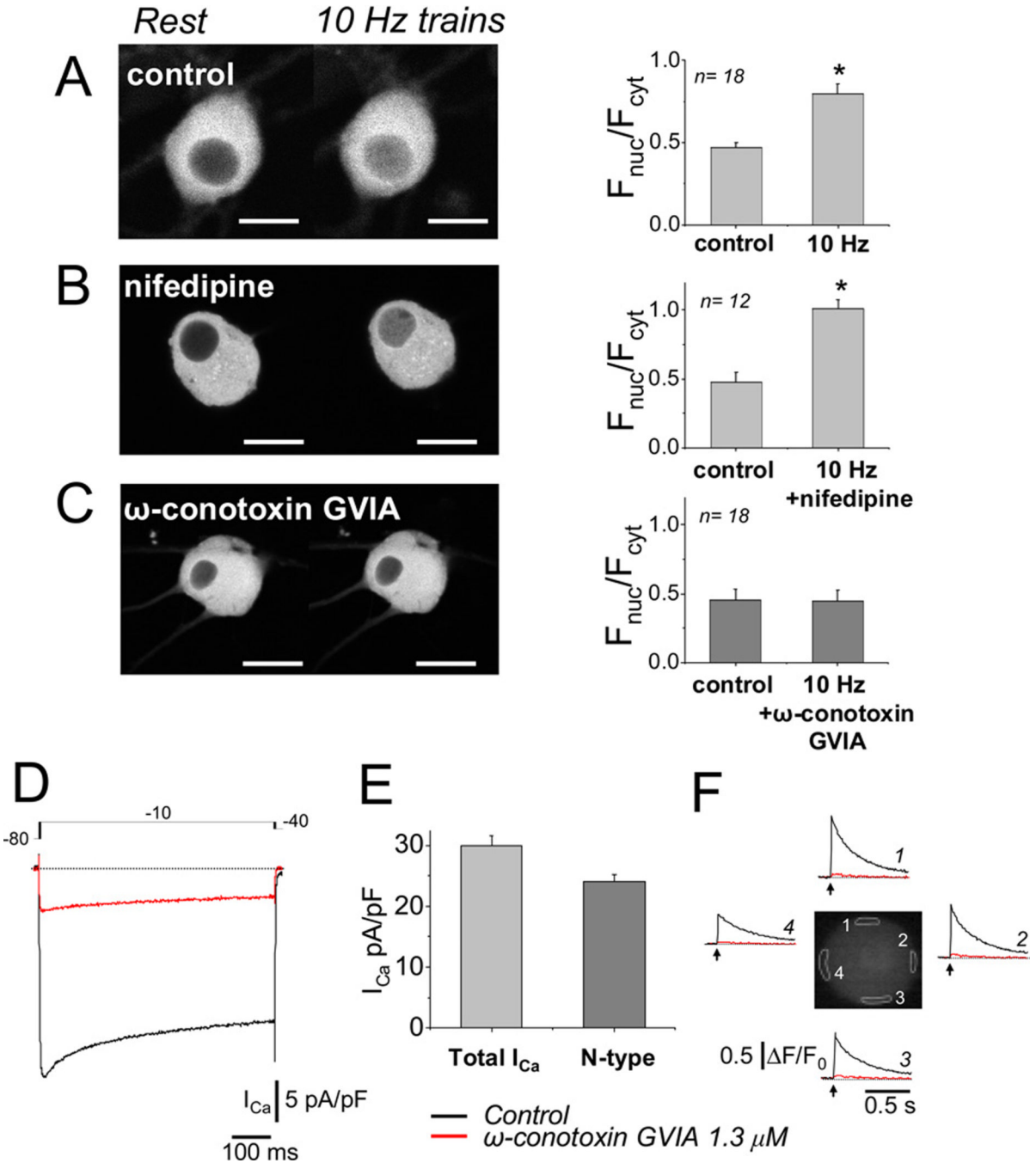

Figure 8.

5 s trains of 10 Hz electrical field stimulation produced an ω-conotoxin GVIA sensitive translocation of NFATc1-CFP from cytosol to nucleus. (A)–(C) Representative images of neurons expressing NFATc1-CFP before (left), and 40 min after the start of electrical stimulation (right) using repetitive application (once every 50 s) of a 5 s train of 10 Hz stimuli in control conditions (A), in the presence of 5μM nifedipine (B; no effect on NFATc1 nuclear translocation), or in the presence of 1.3μM ω-conotoxin GVIA (C), which completely blocked the 10 Hz train stimulation-induced NFATc1 nuclear translocation. Bar plots, nuclear/cytoplasmic ratios (F_{nuc}/F_{cyt}) for each condition. (D) Representative whole cell Ca^{2+} current traces (I_{Ca}), elicited by depolarizing pulses using the voltage protocol

indicated at the top, with 5 mM Ca^{2+} as charge carrier. Application of 1.3 μM ω-conotoxin GVIA blocked ~80% of the total current. (E) Summary of total and N-type (ω-conotoxin-sensitive) Ca^{2+} current density (n = 12 cells). N-type current equaled ~80 % of the total current. (F) An SCG neuron with phasic response was stimulated with single 2ms field stimulus (arrow), and the resulting Ca^{2+} transients, calculated as $\Delta F/F_0$ values, are shown at four peripherally located AOIs (white-highlighted areas in neuron's image). The Ca^{2+} responses were first recorded under control conditions (black traces), and then in the presence of ω-conotoxin added to the Ringer's solution (red traces), which completely blocked the Ca^{2+} transient. A–C from 4 or 5 day cultured SCG neurons expressing NFATc1-CFP. D–F from 3-day cultured SCG neurons.

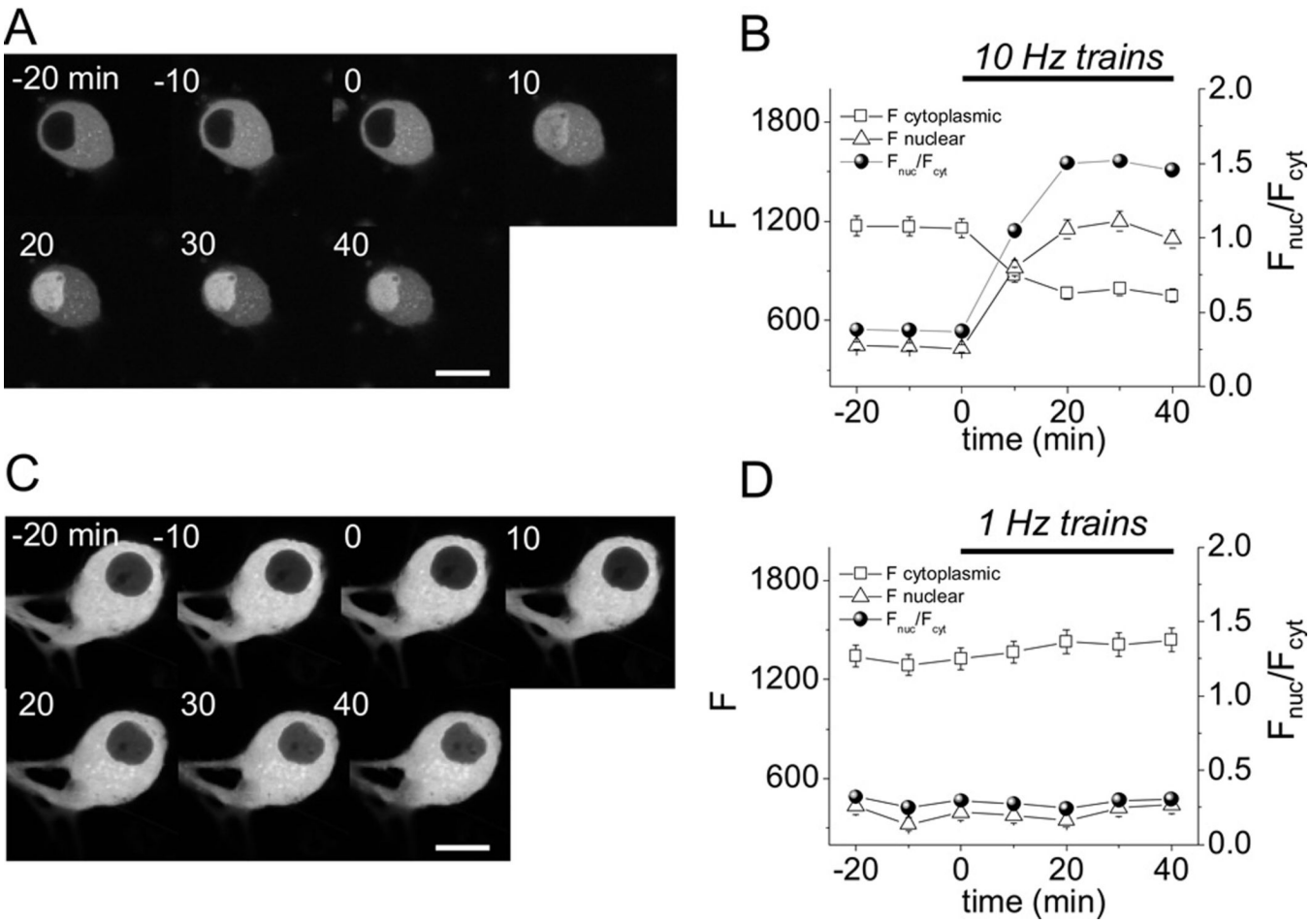

Figure 9.

Time course of NFATc1 nuclear translocation for repetitive 5 s trains of 10 Hz or 1 Hz electric field stimuli. (A) NFATc1-CFP fluorescence images of the same SCG neuron before (−20 to 0 min) and during (0 to 40 min) repetitive electrical field stimulation with 5 s trains of 10 Hz stimuli applied once every 50 s. (B) Time course of cytosolic (open square) and nuclear (open triangle) mean pixel fluorescence (arbitrary units, left scale), and the ratio of nuclear to cytosolic (F_{nuc}/F_{cyt}) mean pixel fluorescence (filled circles, right scale). 10 Hz train stimulation produces a marked redistribution of NFATc1-CFP from cytoplasm to nucleus (n = 12). (C and D), same as A and B, but using 5 s trains of *1 Hz* stimuli applied every 50 s, which produces no appreciable translocation of NFATc1-CFP from cytoplasm to nucleus (n = 8). Neurons were selected to have cytoplasmic fluorescence between 1000 and 1800 to minimize effect on expression levels. Scale bar 10 μm.